AIAA JOURNAL
Vol. 31, No. 7, July 1993

Postbuckling Failure of Composite Plates with Holes

H. H. Lee* and M. W. Hyer†
Virginia Polytechnic Institute and State University, Blacksburg, Virginia 24061

This paper summarizes a study focused on understanding the failure mechanisms present in a plate with a centrally located circular hole loaded in-plane into the postbuckling range of deflections. The study was numerical and experimental in nature and had as a goal the a priori prediction of failure using existing failure data and a stress analysis. The maximum stress failure criterion was used to predict failure and both intralaminar and interlaminar stresses were considered. Four laminates were studied. The phenomenon of modal interaction, or the jumping from one deformed configuration, is discussed. The study concludes that the failure of the $(\pm 45/0/90)_{2S}$ and $(\pm 45/0_2)_{2S}$ laminates is due to fiber compression failure and is predictable. The failure load is, for the most part, independent of response configuration. The $(\pm 45/0_6)_S$ laminate fails due to interlaminar shear along the simple support, while the response and failure of the $(\pm 45)_{4S}$ laminate is governed to a large degree by material nonlinearities and progressive failure.

Introduction

A NUMBER of past research efforts have focused on understanding the postbuckling stiffness of composite plates. To utilize the inherent postbuckling stiffness, the postbuckling strength of composite plates has recently come under examination, both qualitatively and quantitatively. In Ref. 1, the location of failure in solid plates was addressed by examining the strain-energy density, while in Ref. 2 ten criteria were used to predict failure of solid plates. In Ref. 3, analyses were conducted for plates with holes which were compared with experimental work conducted earlier. The issue of the postbuckling of plates and the subsequent failure is important if the stiffness and strength of composite plates are to be used in the design process. This present work continues to quantitatively, and qualitatively, examine the failure issue in some detail.

The plates considered in this study were simply supported along the two opposite vertical side edges and were clamped on the top and bottom edges. The specifics of the geometry, nomenclature, and instrumentation to measure plate response are shown in Fig. 1. The top edge moved uniformly downward with a known displacement u. The bottom edge did not move. The in-plane displacements tangent to the four edges were not specified. Along the two simply supported edges the in-plane normal displacements were not specified either. To account for the fact that no plate is perfectly flat, a small initial out-of-plane deflection was included in the analysis.

The region typically considered for analysis in these situations is the region within four support boundaries, i.e., in Fig. 1 the region within the four dotted lines. An important feature of the present problem, and a feature of all such experiments, was the fact that the plate actually extended beyond the support boundaries. These extensions were necessary to implement the boundary conditions. It was found to be important to include the extensions in the analysis rather than consider the plate to be of dimensions defined by the support boundaries. Thus, the simple-support condition was enforced inward from the actual edge of the plate, there being an extension, or strip, of plate beyond the simple support which terminated with a traction-free edge. On the clamped end similar extensions were within the clamp.

The goal of the present work, then, was to determine the level of in-plane displacement, or alternatively, the level of in-plane load, at the clamped end of the plate that caused the plate to fail. Inherent in this was 1) the accurate prediction of the stresses within the plate, including intralaminar and interlaminar stresses; 2) the definition of failure; and 3) the determination of the location and mode of the failure. With the possibility of a change in the postbuckled configuration to multiple half-waves in the loading direction, interlaminar failure was a candidate failure mechanism.

Approach Used in Study

The numerical portion of the study was based exclusively on the finite element method. Owing to the complex nature of the boundary conditions of the actual plate, i.e., the extensions, no other approach was considered. The finite element formulation used a shear-deformable plate theory; a shear-deformable theory being chosen not because the plates were thick, but rather a shear-deformable theory makes the formulation simpler. Linear elastic response was assumed throughout and the analysis was integrated into a program based on standard procedures[4] and was thoroughly checked for convergence and accuracy relative to simpler nonlinear problems.[5] A Newton-Raphson technique was used with the nonlinear formulation. The calculation of the interlaminar stresses was based on the integration of the equations of elasticity through the thickness of the laminate using the intralaminar stresses as a basis for integration. Integration was done at the element's centroidal Gauss point[6]. The issue of failure was addressed by using the maximum stress criterion and the Gauss point stresses. This criterion was used because it is easy to understand and it relies on simple failure data. To address the issue of the plates deforming into one of several geometric configurations, first the response of the plate deforming with one half-wave in the loading direction was considered, and then the response with two half-waves in the loading direction was considered, the particular response being determined by the initial imperfection used in the analysis. In each case one half-wave perpendicular to the loading direction was used. Four graphite-epoxy laminates, all 16 layers in thickness, were considered. The layups were $(\pm 45/0/90)_{2S}$, $(\pm 45/0_2)_{2S}$, $(\pm 45/0_6)_S$, and $(\pm 45)_{4S}$. Because the anisotropic coefficients[7] for these laminates were quite small, they were assumed to be zero and a quarter-plate analysis was used throughout. Symmetric or antisymmetric conditions, depending on the re-

Presented as Paper 92-2280 at the AIAA/ASME/ASCE/AHS/ASC 33rd Structures, Structural Dynamics, and Materials Conference, Dallas, TX, April 13-15, 1992; received May 5, 1992; revision received Nov. 18, 1992; accepted for publication Nov. 30, 1992.

*Current address: Agency for Defense Development, Yuseong, Taejon, South Korea 305-600. Member AIAA.

†Professor, Department of Engineering Science and Mechanics. Associate Fellow AIAA.

sponse being studied, were assumed along the lines defining the quarter-plate geometry.

The fixture used to load and support the plates was specially built and although it was similar in basic features to those used by other researchers, precautions were taken to assure that at the top and bottom edges the plate specimens and the surface of the fixture contacting the plate edges were very flat. Also, accommodations were made to account for any lack of parallelism between the top and bottom edges. As shown in Fig. 1, the plates themselves were 279 mm square. The outer 12.5 mm on all four edges was used to accommodate the clamped and simple-support conditions. The holes were 75 mm in diameter. Considering the 250 × 250-mm dimensions within the boundaries, the hole diameter to plate-width ratio was 0.3. The specific dimensions studied were dictated somewhat by experimental considerations, and somewhat by the work of other investigators (e.g., Ref. 8), their work serving as a basis for comparison. In the experiments the plates were loaded quasistatically. In-plane and out-of-plane deflections were measured, as were the strains, including back-to-back measurements. Shadow moire measurements of the out-of-plane deflections were made. All quantities measured could be compared with predictions. The laminates were constructed of AS4/3502 graphite-epoxy and the 16 layers were nominally 2.16 mm thick. The elastic properties for a layer of material[7,8] and the failure stresses[9,10] are given in Table 1.

Failure Predictions

With the maximum stress failure criterion, the following five failure parameters can be defined:

$$R_1 = \sigma_1/X_t \qquad \text{when } \sigma_1 \geq 0$$

or

$$R_1 = \sigma_1/X_c \qquad \text{when } \sigma_1 < 0$$

$$R_2 = \sigma_2/Y_t \qquad \text{when } \sigma_2 \geq 0$$

or

$$R_2 = \sigma_2/Y_c \qquad \text{when } \sigma_2 < 0$$

$$R_{12} = |\tau_{12}|/S_{12}, \qquad R_{13} = |\tau_{13}|/S_{13}, \qquad R_{23} = |\tau_{23}|/S_{23}$$

The denominators of these ratios are the failure stresses from Table 1. In the numerical calculations, as the end shortening increases, the values of these five parameters can be calculated as a function of location and end-shortening value. According to the maximum stress criterion, when any of the ratios reaches unity, failure occurs. The mode of failure is defined by the particular ratio that is unity, e.g., $R_{12} = 1$ signifying intralaminar shear failure, $R_2 = 1$ signifying failure transverse to the fiber direction, etc. With such studies one approach is to load the plate until failure occurs in a particular mode, say, the transverse tension mode, at a particular location. The stiffness of the plate at that location is then adjusted to account for this failure and loading continues. Another failure occurs and the stiffness is again adjusted. After a number of these failures and adjustments, failure is said to occur. In the present study the scheme was less involved. Here the stiffnesses were not adjusted when a particular failure occurred, the loading simply continued until fiber failure or interlaminar shear failure occurred. The load when either of these modes occurred was considered the failure load.

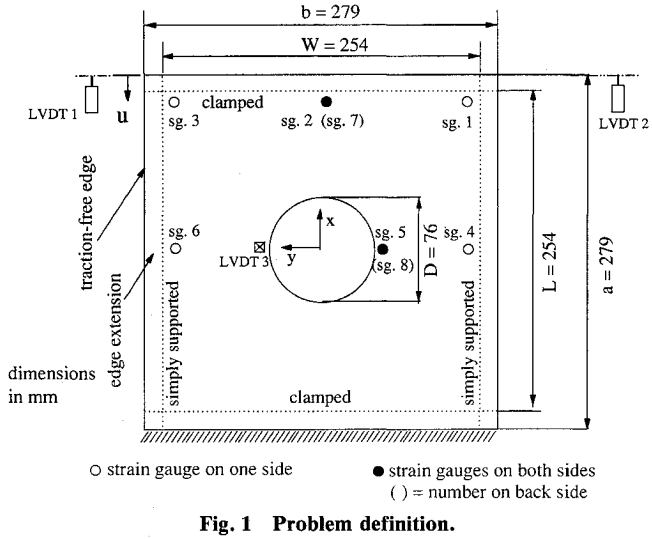

Fig. 1 Problem definition.

Table 1 Material properties

Elastic properties	Strength properties, ksi
$E_1 = 128$ GPa	$X_t = 1.38$ GPa; $X_c = -1.38$ GPa
$E_2 = 11.0$ GPa	$Y_t = 48.3$ MPa; $Y_c = -241$ MPa
$G_{12} = 5.74$ GPa	$S_{12} = S_{13} = 64.8$ MPa
$G_{23} = 2.29$ GPa	$S_{23} = 55.0$ MPa
$\nu_{12} = 0.35$	

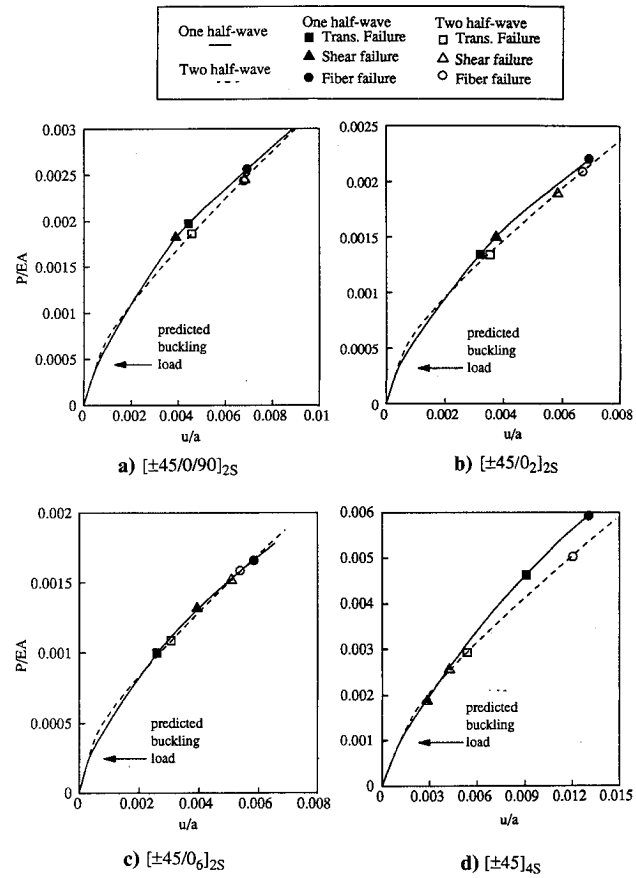

Fig. 2 Predicted load vs end-shortening relations and first failures.

The predicted load-end shortening relations for the four plates are shown in Fig. 2. The loads are nondimensionalized by the load direction modulus E, and the cross-sectional area A, $A = 2.16 \times 279$ mm^2. The end shortening is normalized by overall plate length a, $a = 279$ mm. The values of E are given in Table 2, as are the buckling loads. Buckling-load predictions were made using another finite element formulation developed as part of this study. In each subfigure, the response of a particular plate for the case of one half-wave in the loading direction and the response for the case of two half-waves in the loading direction are shown, with solid and dashed lines, respectively. The magnitude of the imperfection

Table 2 Buckling and failure loads, P/EA[a]

Laminate	E, GPa	Buckling			Failure		
		Numerical	Experimental	Difference	Numerical	Experimental	Difference
$(\pm 45/0/90)_{2S}$	50.9	0.000411	0.000370	−10%	0.00244	0.00253	+4%
$(\pm 45/0_2)_{2S}$	74.5	0.000321	0.000305	−5%	0.00206	0.00200	−3%
$(\pm 45/0_6)_S$	101	0.000245	0.000234	−4%	0.00156	0.00154[b]	−6%
$(\pm 45)_{4S}$	19.8	0.000980	0.000880	−10%	0.00485	0.00359[c]	−26%

[a] $A = 2.16 \times 279$ mm^2.
[b] Interlaminar shear failure at simple-supported edge not predicted.
[c] Poor correlation due to material nonlinearity and progressive failure.

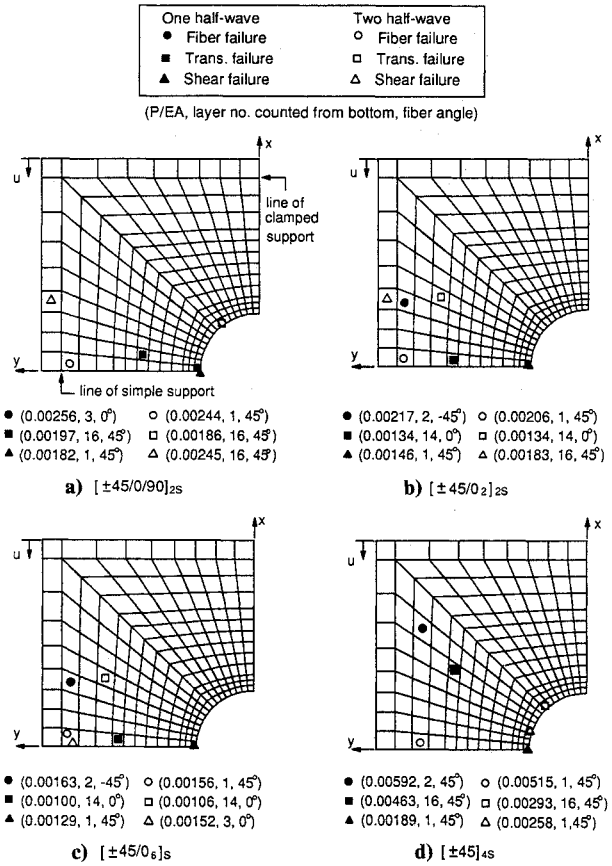

Fig. 3 Predicted first failure locations.

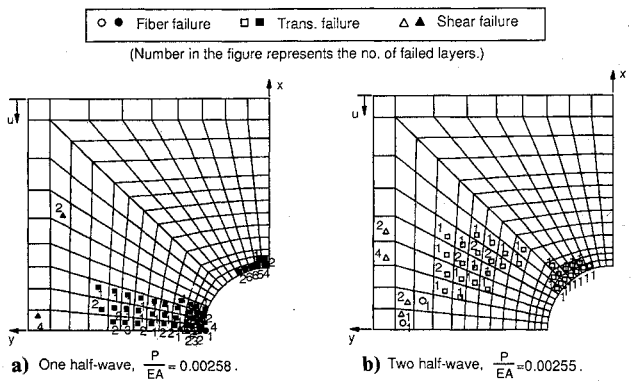

Fig. 4 Predicted failure locations for the $(\pm 45/0/90)_{2S}$ laminate.

was 10% of the plate thickness and, as stated earlier, the shape of the initial imperfection controlled in the analysis whether the plate responded with one half-wave or two. On each load-end shortening relation the loads that correspond to the various failure modes are noted, as is the predicted buckling load. Considering the $(\pm 45/0/90)_{2S}$ laminate, Fig. 2a, with one half-wave in the loading direction (the solid line), as the end shortening increases from zero, the load increases in a linear fashion until the buckling conditions are reached. As the plate is loaded beyond buckling, the stiffness decreases but the plate continues to resist load. At about 4.5 times the buckling load the first in-plane shear failure is predicted to occur, as is indicated by the solid triangle. Figure 3a provides information on the spatial location of this failure, the solid triangle indicating that the location of the first in-plane shear failure is at the net section hole edge. Figure 3a also illustrates the finite element mesh used in the quarter-plate analysis, as well as the locations of the simple supports and the clamping. The numbers associated with the solid triangle in Fig. 3a indicate that the first in-plane shear failure is predicted to occur at $P/EA = 0.00182$ in layer no. 1, a 45-deg layer. With the convention in these figures, the plate is assumed to deflect in the positive z direction (see Fig. 1). Layer no. 1 is located at the negative-most z location. Hence, layer no. 1 is on the innermost concave side of the plate. Referring again to the solid line of Fig. 2a, at a slightly higher load the first transverse failure is predicted to occur at the location shown by the solid square in Fig. 3a. Finally, at about six times the buckling load, the first fiber compression failure is predicted to occur at the net-section hole edge. This failure occurs in the first 0-deg layer (layer no. 3) on the concave side of the plate and is due to the stress concentration effect associated with the in-plane loading of a plate with hole. This event is considered failure of the plate and the associated load level is considered the failure load. Although first failures for each particular mode have been emphasized, in reality intralaminar shear and transverse tension failures are widespread by the time the first fiber failure occurs. Figure 4a illustrates predicted failure locations for the $(\pm 45/0/90)_{2S}$ laminate in the one-half-wave configuration at a load slightly above the first fiber failure load. The predicted locations of all of the intralaminar and transverse failures at the fiber failure load level are indicated, as is the number of layers that have failed.

If the $(\pm 45/0/90)_S$ plate responds in two half-waves, the dashed line of Fig. 2a, the first transverse tensile failure, the open square, is predicted to occur at about the same load level it did for the one-half-wave configuration. As shown in Fig. 3a, the location, however, is predicted to be different. For the two-half-wave case, intralaminar shear failure and fiber compression failure are predicted to occur at the same load level. Interestingly enough, the load level for fiber compression failure is about the same for the two-half-wave configuration as it is for the one-half-wave configuration. However, the location of fiber failure for the two-half-wave configuration is at the net section along the simple support rather than at the hole edge. In addition, fiber failure occurs in the first 45-deg layer on the concave side, rather than the first 0-deg layer on the concave side. The predicted failure locations at a load slightly greater than the fiber failure load level for the two-half-wave configuration is shown in Fig. 4b. It should be mentioned that for the $(\pm 45/0/90)_{2S}$ plate, interlaminar shear was not an issue. Those stresses were low. It should also be noted that intralaminar shear failures were predicted to occur outside the simple support. As it is the lower of the two fiber failure loads, the value of $P/EA = 0.00244$ for the two-half-

wave configuration fiber failure load was taken as the failure load for the $(\pm 45/0/90)_{2S}$ laminate.

The response and first failure predictions for the $(\pm 45/0_2)_{2S}$ plate are shown in Figs. 2b and 3b. As can be seen in Fig. 2b, the first transverse tension failure load level is independent of the deformed configuration (a coincidence) and the first intralaminar shear failure load level is dependent on the configuration, and the first compression failure load level is predicted to be nearly independent of configuration. For the one- and two-half-wave configurations, the locations of the various first fiber failures are again different. Referring to Fig. 3b, in both configurations first fiber failure occurs along the simply supported edge, failure occurring at the net section for the two-half-wave configuration and slightly away from the net section for the one-half-wave configuration. Although it is not shown here, it is interesting to note that more intralaminar shear failures are predicted to occur outside the simple support for this laminate than for the previous one, particularly considering that half of the layers (8) were predicted to fail in some locations. The predicted failure load of the $(\pm 45/0_2)_{2S}$ laminate is higher than the predicted failure load of the $(\pm 45/0/90)_{2S}$ laminate. Again, interlaminar shear failure was not a factor, even with the two-half-wave configuration. The value $P/EA = 0.00206$ was considered the failure load for this laminate.

The predicted results for the $(\pm 45/0_6)_S$ and $(\pm 45)_{4S}$ laminates make up Figs. 2c–2d and 3c–3d. For the $(\pm 45/0_6)_S$ laminate, the first fiber compression failure is predicted to occur along the simple support, independent of the configuration, being away from the net section for the one-half-wave configuration and being at the net section for the two-half-wave configuration. The fiber failure load level for the two configurations is about the same, as has been the case for the two previous laminates. Also as with the previous cases, although it is not shown here, at the first fiber failure load level transverse tension and intralaminar shear were predicted to be widespread, including some failures outside the simple support. With the 12 0-deg layers in this laminate, transverse tensile or shear failure through all 12 layers at various locations is not surprising. Interlaminar failure was not an issue and a value of $P/EA = 0.00156$ was considered the failure load of this laminate. As will be seen shortly, the predictions for the $(\pm 45/0_6)_S$ laminate overlooked an important factor.

The predictions for the $(\pm 45)_{4S}$ laminate are somewhat different than for the other laminates. Although fiber compression failure can be predicted from the analysis, intralaminar shear failure was predicted in all 16 layers in both the one-half-wave and the two-half-wave configurations at load levels less than the first fiber failure level. Shear failures which encompassed the entire thickness of the plate were felt to represent failure of the plate. This occurred at the locations outside the simple supports at a value of $P/EA = 0.00485$ in the one-half-wave configuration. (This does not correspond to any particular symbol on Fig. 2d.) Interlaminar stresses were low.

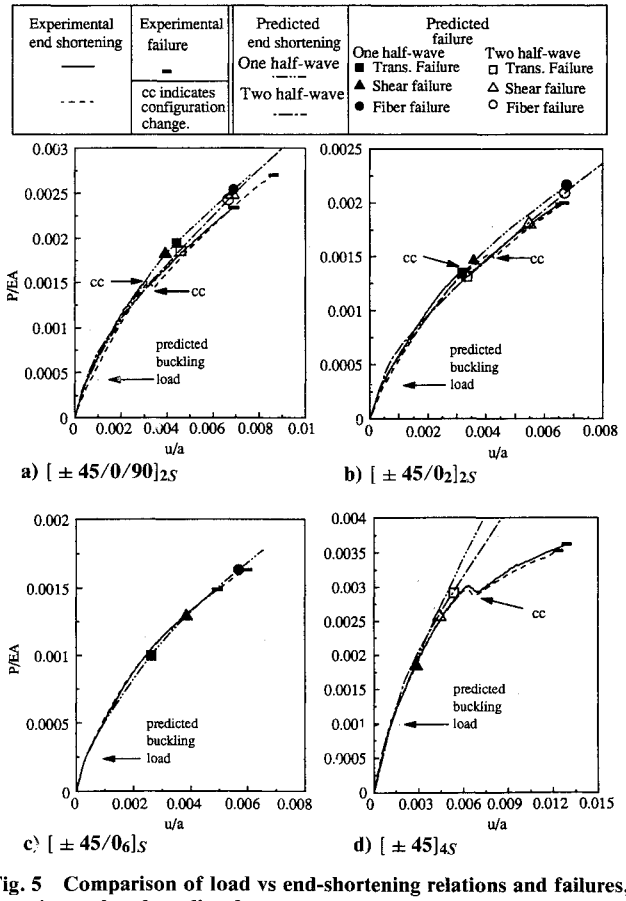

Fig. 5 Comparison of load vs end-shortening relations and failures, experimental and predicted.

Experimental Results and Comparison with Predictions

With four laminates, three displacement transducers, multiple strain gauges, shadow moire photographs, postfailure results for each test, and a replicate test for each laminate, there was a large amount of information that came from the experimental phase of this study. To report it all here is not possible, nor even necessary. Here the results for just one laminate, the $(\pm 45/0/90)_{2S}$, will be presented. After this laminate is discussed, particular aspects of the results for the other laminates which deviated significantly from predictions, or which deviated significantly from the results for the $(\pm 45/0/90)_{2S}$ laminate, will be emphasized. Details of the test results for other laminates can be found in Ref. 5.

Results for the $(\pm 45/0/90)_{2S}$ Plates

Although this study focused on postbuckling, it is important to compare predicted and measured buckling loads. Experimental buckling loads were determined from the load vs end-shortening relations, using the intersection of two straight lines, one tangent to the initial prebuckling path and the other tangent to the initial postbuckling path. Comparisons between predicted and measured results for the $(\pm 45/0/90)_{2S}$ laminate, as well as the other laminates, are shown in Table 2. The table shows the average buckling loads for the two replicate specimens, the numerical prediction, and the difference between the two. As expected, the measured buckling loads were lower than the predicted levels, there being about a 10% difference for the $(\pm 45/0/90)_{2S}$ laminate.

The measured load vs end-shortening relationships for the two $(\pm 45/0/90)_{2S}$ plates tested are compared with predictions in Fig. 5a. The predictions for one half-wave and two half-waves in the loading direction are shown. The predictions were shown in Fig. 2a and they are simply repeated in Fig. 5a. The line styles, however, have been changed. The failure symbols are the same. (A better view of the line styles and symbols is available in Fig. 5d, where the 4 lines are more spread out.) As can be seen, one specimen (the dashed line) deviated more from the ideal straight-line prebuckling path at a lower load than the other specimen (the solid line). For both plates, as the load increased from zero, the plate deformed with one half-wave in the loading direction. At a load level of $P/EA = 0.0015$, both plates experienced a sudden change in configuration to two half-waves in the loading direction. The configuration change is marked with "cc" on the figures. The repeatability of this change in configuration with both specimens was remarkable. With continued loading, the plate responded in the two-half-wave configuration, the response being somewhat softer than the prediction. One plate failed at $P/EA = 0.00234$ and the other plate failed at $P/EA = 0.00271$, the average value being $P/EA = 0.00253$. The predicted failure load was $P/EA = 0.00244$, there being about a 4% difference between predicted and the average measured value. As mentioned earlier, fiber compression was the pre-

dicted mode, the predicted location for the two-half-wave configuration being at the net section along the simply supported edge at the net section.

Figure 6a provides a different view of the plate response. The load vs the net-section hole edge out-of-plane displacement responses, both predicted and measured, are illustrated. As can be seen, with the configuration change the out-of-plane response suddenly decreases. Theoretically, for the quarter-plate analysis, the out-of-plane displacement of the hole edge is zero in the two-half-wave configuration.

It should be noted that the load vs end-shortening relations from the experiments were determined by averaging the responses of two displacement transducers measuring the in-plane end-shortening displacements along the left and right simply supported edges. For all four laminates these two responses were quite close to each other, indicating good uniformity of the in-plane displacement across the width of the plate.

The strain-gauge measurements compared well with the numerical predictions. Large increases in strains (doubling of values) at certain locations of the plate were observed when the configuration changed from one half-wave in the loading direction to two. Figure 7 shows the predicted and measured responses of two back-to-back gauges at the net-section hole edge. Gauge 5 is on the $+z$ side of the plate, while gauge 8 is on the $-z$ side of the plate. At the configuration change, gauge responses decreased dramatically, just as other gauge responses, e.g., gauges 2 and 7 (see Fig. 1), increased.

Based on the preceding figures, it can be said with a high degree of confidence that the deformations of the $(\pm 45/0/90)_{2S}$ plates, both in terms of displacements and strains, can be predicted very well. More importantly, it can be said that the failure load for the $(\pm 45/0/90)_{2S}$ plates can also be predicted quite closely. In that regard, a failed $(\pm 45/0/90)_{2S}$ plate, still in the loading fixture, is shown in Fig. 8. The failure of the other $(\pm 45/0/90)_{2S}$ plate looked identical. Failure occurred at the net section along the left simple support, as indicated by the dark area in the photograph. (The plates were painted white to enhance the shadow moire images.) As indicated by the open circle in Fig. 3a, failure was predicted to occur at this specific location. Table 2 summarizes the predicted and observed average failure loads and indicates, as stated before, the difference between for the $(\pm 45/0/90)_{2S}$ laminates is about 4%.

Results for the $(\pm 45/0_2)_{2S}$ Plates

The results for the $(\pm 45/0_2)_{2S}$ plates were quite similar to the results for the $(\pm 45/0/90)_{2S}$ plates. The predicted and observed load vs end-shortening relations were close, as shown in Fig. 5b. The two $(\pm 45/0_2)_{2S}$ plates did not, however, change configuration at the identical load level. The difference in the configuration change load levels between the two plates was about 15%. However, the plates failed at very similar load levels. As can be seen in Table 2, the average failure load for

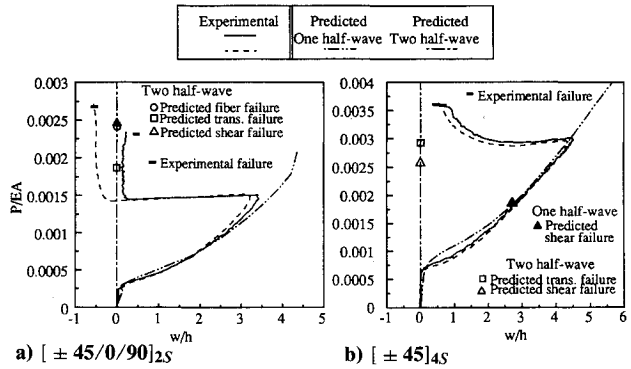

Fig. 6 Comparison of load vs out-of-plane deflections and failures, experimental and predicted.

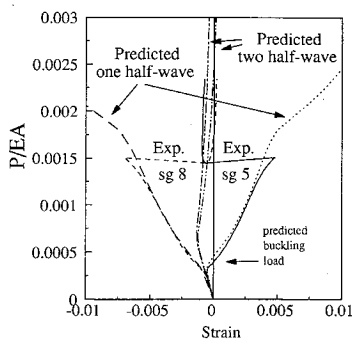

Fig. 7 Comparisons between predicted and measured strains.

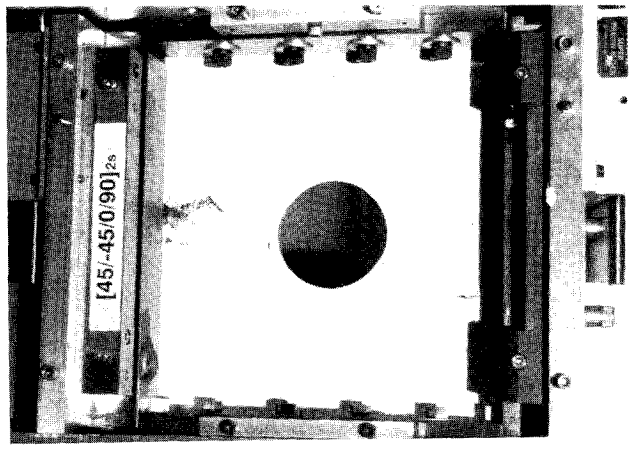

Fig. 8 A failed $(\pm 45/0/90)_{2S}$ laminate.

the replicate plates was only 3% lower than predicted and the predicted failure mode was observed.

Results for the $(\pm 45/0_6)_S$ Plates

The $(\pm 45/0_6)_S$ laminate did not exhibit a change to the two-half-wave configuration. Both replicate plates continued to respond in the one-half-wave configuration, the correlation between predictions and measurements being very good. There was about a 12% difference in the experimentally measured failure loads for the two replicate specimens. The load vs end shortening is shown in Fig. 5c, there being only the one half-wave predicted end-shorten relation shown. The figure indicates that the correlation between predicted and observed failure loads was good. However, that comparison does not tell the whole story. These plates did not fail due to fiber failure. These plates actually failed due to interlaminar shear stress along the simply supported edges, the interlaminar shear stress τ_{yz} being responsible for failure. Within the 12 0-deg layers in this laminate, $\tau_{yz} = \tau_{23}$ and it appears the interlaminar shear stress τ_{23} was the important principal material system stress component, that stress component being highest at the laminate midplane at the simply supported edge. A significant level of τ_{23} was computed there but the value of R_{23} was not such as to predict failure. However, it appears that clustering of the 12 0-deg layers resulted in a lower-than-anticipated capacity of the laminate as regards τ_{23}. Using the numerical analysis to compute maximum value of interlaminar stress τ_{23} at the load corresponding to the failure load, a value of 13.8 MPa for the failure stress S_{23}, rather than the 55.0 MPa of Table 1, appeared to be more applicable to the clustered layers. One plate failed along one simple support, and the other plate failed along both simple supports.

Results for the $(\pm 45)_{4S}$ Plates

At high load levels the observed and predicted responses of the $(\pm 45)_{4S}$ plates deviated considerably. The load vs displace-

ment relations are shown in Figs. 5d and 6b. The plates exhibited a configuration change but the transition was slow. The failure loads for the two plates were below the predicted level for all 16 layers failing outside the simple supports due to intralaminar shear, this prediction being discussed in connection with Figs. 2d and 3d. However, the plates did fail due to what appeared to be excessive intralaminar shear, one plate failing at one simple support, the other failing at both simple supports. It is felt that the high level of nonlinear material behavior, specifically softening, that normally characterizes the intralaminar shear stress vs shear strain relation of fiber-reinforced material was responsible for the observed behavior. With the stress levels building as the plate began to change configuration, the softening effect in this plate, which had no 0-deg layers, could well have reduced the severity of the sudden change from one configuration to the other. Clearly both plates began the usual sudden change from the one-half-wave configuration to the two-half-wave configuration at P/EA of about 0.003. However, as the load continued to increase, although the change in configurations was quick at first, it tended to slow down. The in-plane deflections (the end shortening) increased dramatically. Both of these trends indicate a softening effect.

Overall Summary and Concluding Comments

In the context of the study, it can be concluded that 1) postbuckling failure can be predicted; and 2) despite the plate deforming into the two-half-wave configuration, interlaminar stresses are not necessarily an issue.

The case for which interlaminar stresses were an issue involved the one-half-wave configuration and a laminate that might not be considered practical, i.e., the $(\pm 45/0_6)_S$ laminate. For the two laminates in common usage, the $(\pm 45/0/90)_{2S}$ and the $(\pm 45/0_2)_{2S}$ laminates, the prediction of postbuckling response and failure is in hand. This statement is made in the context of square planform plates with a specific hole geometry. Plates with smaller holes or no holes may have different failure characteristics. Plates with larger holes most likely behave similarly to the ones studied here. However, those points need to be investigated. The investigation of these points is important because the configuration change characteristics may depend to some degree on hole size. In addition, for the case of no hole, material in the geometric center of the plate may indeed experience high interlaminar stresses if the plate deforms into the two-half-wave configuration. This all relates to a more underlying issue, namely that of actually being able to predict the configuration change. Predicting when and if the configuration will change, what parameters control it, whether or not it is necessary to prevent the change in the context of failure, and so forth, are all facets to this underlying issue. They must be addressed before designers can truly feel comfortable with design in the postbuckling range of response.

Finally, it is conceivable that a $(\pm 45)_{4S}$ laminate would find application, and it is clear from the lack of agreement between the predicted and the experimental results here that the nonlinear material behavior of such a laminate must be fully accounted for.

Acknowledgment

This study was supported by Grant NAG-1-901 from the Aircraft Structures Branch of the NASA-Langley Research Center to Virginia Tech. The grant monitor was M. P. Nemeth of that Branch. The technical and financial support are appreciated.

References

[1]Noor, A. K., Starnes, J. H., Jr., and Waters, W. A., Jr., "Numerical and Experimental Simulations of the Postbuckling Response of Laminated Anisotropic Panels," AIAA Paper 90-0964CP, April 1990.

[2]Turvey, G. J., and Osman, M. Y., "Exact and Approximate Linear and Nonlinear Initial Failure Analysis of Laminated Mindlin Plates in Flexture," *Composite Structures*, edited by I. H. Marshall, Elsevier Applied Science, New York, 1989, pp. 133–171.

[3]Engelstad, S. P., Reddy, J. N., and Knight, N. F., "Postbuckling Response and Failure Prediction of Flat Rectangular Graphite-Epoxy Platers Loaded in Axial Compression," AIAA Paper 91-0910CP, April 1991.

[4]Reddy, J. N., *An Introduction to the Finite Element Method*, McGraw-Hill, New York, 1984, Chap. 4.

[5]Lee, H. H., and Hyer, M. W., "Postbuckling Failure of Composite Plates with Central Holes," Center for Composite Materials and Structures Rept. CCMS 92-07, Virginia Polytechnic Inst. and State Univ., Blacksburg, VA, 1992.

[6]Chadhuri, R. A., and Seide, P., "An Approximate Semi-Analytical Method for Prediction of Interlaminar Shear Stresses in an Arbitrarily Laminated Thick Plate," *Computers and Structures*, Vol. 25, No. 4, 1987, pp. 627–636.

[7]Nemeth, M. P., "Importance of Anisotropy on Buckling of Compression Loaded Symmetric Composite Plates," *AIAA Journal*, Vol. 24, Nov. 1986, pp. 1831–1835.

[8]Nemeth, M. P., "Buckling Behavior of Compression Loaded Symmetrically Laminated Angle-Ply Plates with Holes," *AIAA Journal*, Vol. 26, No. 3, 1988, pp. 330–336.

[9]Burns, S. W., Herakovich, C. T., and Williams, J. G., "Compressive Failure of Notched Angle-Ply Composite Laminates: Three-Dimensional Finite Element Analysis and Experiment," Center for Composite Materials and Structures Rept., CCMS 85-11, Virginia Polytechnic Inst. and State Univ., Blacksburg, VA, 1985.

[10]Berg, J. S., and Adams, D. F., "An Evaluation of Composite Material Compression Test Methods," *Journal Composites Technology and Research*, Vol. 11, No. 2, 1989, pp. 41–46.